

Structure of Binary Quantum Clusters

Charusita Chakravarty

Department of Chemistry, Indian Institute of Technology-Delhi, Hauz Khas, New Delhi 110016, India
(Received 20 January 1995)

Fourier path integral Monte Carlo simulations are used to demonstrate that in isotopically mixed clusters mass differences can lead to a purely quantum analog of classical binary phase separation. A parametric multistage sampling method is developed to simulate such systems, and results are presented for the strongly quantum mechanical p-H₂/o-D₂ and the quasiclassical ²⁰Ne/²²Ne binary clusters.

PACS numbers: 36.40.-c, 61.20.Ja, 64.75.+g

The analog of the bulk melting transition in clusters has attracted considerable attention and led to a better understanding of phase transitions and thermodynamics in small, finite systems [1,2]. The cluster equivalent of phase separation in binary fluids has been recently investigated using classical simulation methods [3] and is found to be significantly modified in a finite cluster by the presence of a free surface and the small system size.

In this Letter, we examine a purely quantum analog of the species segregation phenomenon observed in classical binary clusters. An isotopic mixture of particles *A* and *B* will appear to be homogenous when the equilibrium properties are examined in the classical limit. The extent of quantum delocalization will, however, depend on the particle mass and result in different effective interaction potentials being perceived by the two species. This is exemplified by the different zero-point energies and mean pair separations of the *A-A*, *A-B*, and *B-B* dimers. As a consequence, a quantum isotopic mixture will display many of the characteristic features of a classical binary mixture. Decreasing quantum delocalization with increasing temperature will act, in addition to the usual entropic factor, to promote mixing with a rise in temperature. Isotopic quantum mixtures have been previously examined in the context of low temperature ³He-⁴He mixtures; for example, ³He impurity states in ⁴He films and clusters [4,5]. In this Letter, we consider isotopically mixed Lennard-Jones (LJ) clusters. Particle masses, potential parameters, and temperatures are chosen to ensure that effects due to quantum mechanical exchange of identical particles are negligible. Quantum effects associated with different isotopic species are then indexed by the thermal de Broglie wavelength relative to the Lennard-Jones length parameter σ , $\lambda_T = \sqrt{\hbar^2/mkT}\sigma^2$, at the same reduced temperature kT/ϵ where ϵ is the well depth parameter.

Consider an isotopically mixed cluster of n_A and n_B particles of masses m_A and m_B , respectively, such that $n = n_A + n_B$. If $m_A < m_B$, then quantum delocalization effects will be greater for species *A* than for *B* and effectively reduce the strength of the *A-A* pair interactions relative to the *A-B* and *B-B* interactions (cf. zero-point energies of dimers). Consequently, one would expect a higher concentration of the more massive (or more

strongly bound) species towards the cluster interior. Such behavior is analogous to that of classical LJ binary clusters with $\epsilon_{AA} < \epsilon_{AB} < \epsilon_{BB}$ and $\sigma_{AA} > \sigma_{AB} > \sigma_{BB}$, which are expected to form "spherically coated" clusters [3]. Structural parameters for monitoring the segregation of the two species into surface and core sites are defined here. The radial density profiles $d_A(R)$ and $d_B(R)$ are defined as the probability of finding a particle of species *A* or *B*, respectively, at a distance *R* from the center of the cluster. The average radii of the two subclusters R_A and R_B are defined as $\int R d_A(R) dR$ and $\int R d_B(R) dR$, respectively. Two particles are classed as nearest neighbors if they lie within a distance of 1.5σ , and the average number of nearest neighbors is denoted by N . The average number of nearest neighbors for particles of species *A* (*B*) is N_A (N_B); clearly if species *A* is concentrated in the core, then $N_A > N_B$. The number of nearest neighbors of a given particle of species *A* (*B*) which belong to the same species *A* (*B*) is a measure of local homogeneity and is labeled f_A (f_B). Additional segregation parameters μ and ν are defined as $\mu = n|R_A - R_B|/(n_A R_A + n_B R_B)$ and $\nu = n|f_A - f_B|/(n_A f_A + n_B f_B)$. In the classical limit, as well as when $m_A = m_B$, both μ and ν must be zero.

To simulate quantum clusters at finite temperatures, a Fourier path integral Monte Carlo (FPIMC) scheme with partial averaging is used (see Refs. [6–8] for details). The Monte Carlo variables are the spatial coordinates of the particles \mathbf{x} and an auxiliary set of Fourier coefficients \mathbf{a} . The partition function Q for the quantum system can be written as $Q = \int d\mathbf{x} d\mathbf{a} \exp\{-S(\mathbf{x}, \mathbf{a}; \beta, m_A, m_B)\}$, where S is the Euclidean action associated with the cyclic quantum path defined by \mathbf{x} and \mathbf{a} . S depends parametrically on the inverse temperature, $\beta = 1/k_B T$, m_A , and m_B . When *A* and *B* are distinct species, it is necessary to attempt occasional MC moves that interchange the quantum paths of particles of different mass to equilibrate the system efficiently. Such path swapping moves are accepted relatively frequently when $\Delta m = |m_B - m_A|$ is small, but for large Δm these moves have nearly zero acceptance probability.

A MC procedure is described for systems where m_A and m_B are such that path swapping moves have a negligible

acceptance ratio at a given β . In such situations, a reference system must be defined that is identical to the original system in all respects except that the particle masses m_A^0 and m_B^0 are chosen so that equilibration using path-swapping moves is possible. A set of N_R configurations, $X_R = \{\mathbf{x}, \mathbf{a}\}$, are stored from a FPIMC simulation of the reference system. Now consider a FPIMC simulation of the system of interest with the parameters β , m_A , and m_B . Let X be the k th configuration in the Markov chain generated by the standard Metropolis procedure. After these k steps, let X_R be a trial configuration randomly selected from the stored reference distribution; such a trial move will be termed a jump move. Since X_R belongs to the reference distribution with a weight proportional to $e^{-S_R(X_R)}$, the transition matrix element for a jump move going from X to X_R is given by $T(X|X_R) = e^{-S_R(X_R)}$ where $S_R(X)$ is the Euclidean action of configuration X in the reference distribution. The transition probability for the reverse move is given by $T(X_R|X) = e^{-S_R(X)}$. With this choice of transition probabilities and maintaining the detailed balance condition, it can be shown that a jump move must be accepted with probability, $p = \min\{1, q(X|X_R)\}$ where $q(X|X_R) = [e^{-S_R(X)} e^{-S(X_R)}] / [e^{-S_R(X_R)} e^{-S(X)}]$. Thus, standard MC moves combined with occasional jump moves can be used to equilibrate the system of interest. In general, it may be necessary to consider one or more intermediate distributions i with parameters m_A^i , m_B^i , and β as bridging distributions between the reference system and the actual system. To summarize the above MC procedure, a simple parametric shift is used to generate a relatively ergodic reference distribution; the less ergodic system of interest may then be equilibrated by coupling or latching on to this reference distribution. This procedure has therefore been termed "parametric multistage sampling" in the remainder of this Letter and is conceptually similar to the jump-walking algorithm [9].

Two specific Lennard-Jones systems have been chosen for the simulations: (i) para-H₂/ortho-D₂ and (ii) ²⁰Ne/²²Ne isotopically mixed clusters. The Lennard-Jones parameters for neon are $\epsilon = 35.6$ K and $\sigma = 2.745$ Å. At low temperatures, p-H₂ and o-D₂ molecules occupy the $J = 0$ rotational state and can be treated as spinless bosons with isotropic interaction potentials. The effects of identical particle exchange are unimportant above 2 K [10]. For pure p-H₂ and o-D₂ clusters, a Lennard-Jones potential ($\epsilon = 34.2$ K, $\sigma = 2.96$ Å) is found to reproduce quite well the PIMC results obtained with the more accurate Silvera-Goldman potential [9,11]. Therefore at low temperatures, p-H₂ and o-D₂ clusters can be treated as atomic LJ clusters with atomic masses of 2 and 4, respectively.

In all the simulations reported here, the overall acceptance probability in the MC runs was ≈ 0.5 and the run lengths N_{MC} were 10^6 . At 2.5 K, 16 Fourier coefficients per degree of freedom for neon and 24 for the p-H₂/o-D₂

clusters were required to ensure adequate convergence. Acceptance ratios for path swapping moves were ≈ 0.5 for the ²⁰Ne/²²Ne system even at 2 K.

Path swapping moves had virtually zero acceptance probability for (p-H₂)_{*n*}(o-D₂)_{*m*} clusters in the temperature range from 2 to 6 K; it was therefore necessary to use the parametric multistage sampling method. At 2.5 K, the reference system had $m_A^0 = 2.7$ and $m_B^0 = 4.0$ amu with 10% acceptance probability for path swapping moves; the stored distribution had 10^4 configurations. An intermediate distribution with $m_A^1 = 2.3$, $m_B^1 = 4.0$ amu was then equilibrated by attempting jump moves with a probability $P_J = 0.05$. The total number of jump moves accepted was kept less than 70% of the number of stored configurations. 10^4 configurations were stored from this simulation and used to equilibrate the final system of interest ($m_A = 2, m_B = 4$) with P_J and a_J values of 0.025 and 0.12, respectively. At 5 K, the initial reference distribution parameters were $m_A^0 = 2.2$, $m_B^0 = 3.3$, and the intermediate distribution had parameters $m_A^1 = 2.0$, $m_B^1 = 3.5$.

Results are first presented for the simplest scenario of a single impurity atom in a cluster since it provides valuable insight into the mass segregation process. An effective potential $V_{\text{eff}}(R)$ experienced by a tagged atom i at a distance R from the center of the cluster is defined as $V_{\text{eff}}(R) = \langle \sum_{j \neq i} v_{ij} \rangle$ where $\langle \dots \rangle_{MC}$ denotes the average over the MC run, v_{ij} is the pair interaction between the tagged atom i and any other atom j , and atom i is constrained to lie between R and $R + \Delta R$. Two cluster sizes were considered, A(o-D₂)₁₂ and A(o-D₂)₁₇, where the fictitious impurity atom A was an isotope of mass $m_A = 3$ or 5 amu. These choices of m_A serve to exemplify the qualitative difference between light and heavy impurities and allow for equilibration using path swapping moves at 2.5 K. Figure 1(a) shows that $V_{\text{eff}}(R)$ decreases with R reflecting the increase in the number of nearest neighbors in the interior of the cluster. The detailed structure of the $V_{\text{eff}}(R)$ curve reflects the overall cluster structure. Figure 1(a) shows the $V_{\text{eff}}(R)$ curves only for $m_A = 5$; the curves for $m_A = 3$ were very similar and are therefore not shown. It should be noted, however, that for $m_A = 3$, $V_{\text{eff}}(R)$ could be determined reliably only for R greater than 5 bohr; statistical errors in the effective potential for regions where $d(R)$ is small tend to be large and are not plotted in Fig. 1(a). In contrast, Figs. 1(b) and 1(c) show the dramatic difference between density profiles, $d_A(R)$ for the light and heavy impurity. This behavior can be qualitatively understood by considering a single quantum particle in the one-dimensional effective potential; the heavier the quantum particle, the more localized it will be in regions of low potential energy. To study the effect of different $n:m$ ratios, three sets of (p-H₂)_{*n*}(o-D₂)_{*m*} clusters with $n + m = 18$ were simulated using the multistage sampling procedure described previously. The results, along with those for (o-D₂)₁₈ and (p-H₂)₁₈, are shown in Table I.

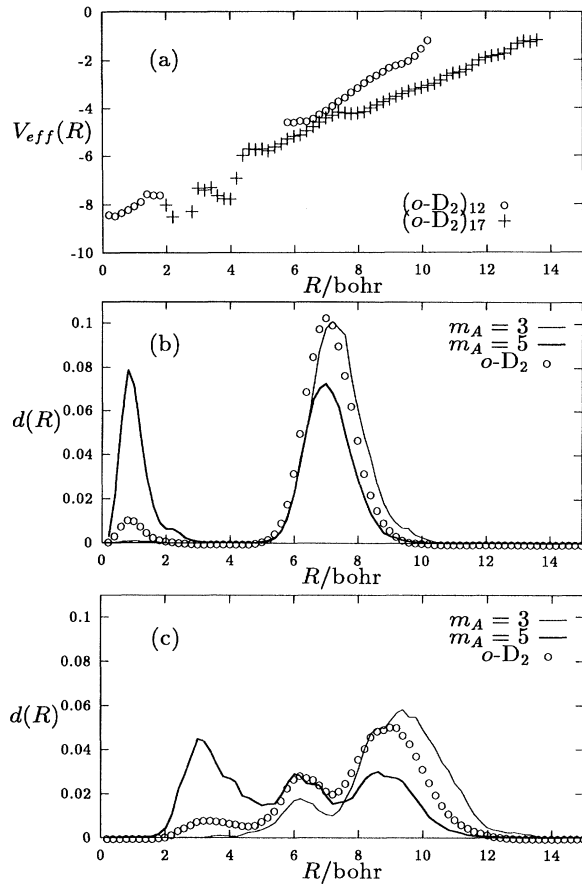


FIG. 1. Isotopic impurity A of mass m_A in an $(\text{o-D}_2)_n$ cluster. (a) Effective potential, $V_{\text{eff}}(R)$, experienced by an isotopic impurity in the $A(\text{o-D}_2)_{12}$ and $A(\text{o-D}_2)_{17}$ cluster with $m_A = 5$. Note that $V_{\text{eff}}(R)$ values for R such that $d_A(R)$ is very small are not shown. (b) Radial density profiles, $d(R)$, for $m_A = 3$ and 5 amu in an $A(\text{o-D}_2)_{13}$ cluster. The dotted line corresponds to the density profile for the o-D_2 subcluster when $m_A = 5$ amu. (c) Radial density profiles, $d(R)$, for $m_A = 3$ and 5 amu in an $A(\text{o-D}_2)_{17}$ cluster. The dotted line corresponds to the density profile for the o-D_2 subcluster when $m_A = 5$ amu.

The preponderance of p-H_2 molecules on the cluster surface is clearly shown by the density profiles in Fig. 2 as well as by the structural parameters given in Table I [12]. Note that $(\text{p-H}_2)_9(\text{o-D}_2)_9$ was simulated at both 2.5 and 5 K; while the cluster is visibly less structured at 5 K, the segregation effect is striking at both temperatures. To provide a comparison, quasiclassical simulations at 5 K using

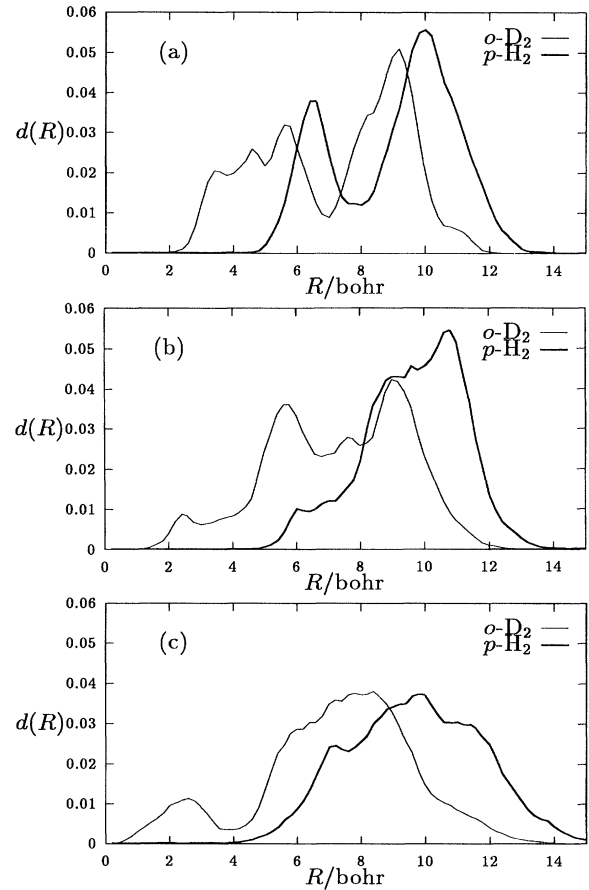


FIG. 2. Radial density profiles, $d(R)$, for the two isotopic species in (a) $(\text{p-H}_2)_9(\text{o-D}_2)_9$ at 2.5 K. (b) $(\text{p-H}_2)_5(\text{o-D}_2)_{13}$ at 2.5 K. (c) $(\text{p-H}_2)_9(\text{o-D}_2)_9$ at 5.0 K.

a quadratic Feynman-Hibbs potential [13] for $(\text{p-H}_2)_9(\text{o-D}_2)_9$ provided $R_A = 1.32\sigma$ and $R_B = 1.48\sigma$ and $N_A = 7$ and $N_B = 6$, where $m_A = 4$ and $m_B = 2$ amu. It would appear that such approximate simulations capture the basic species segregation effect but not the full extent of quantum delocalization. Consequently, it is interesting that the quasiclassical simulation for the 55-particle $(\text{p-H}_2)_{42}(\text{o-D}_2)_{13}$ cluster gives $R_A = 1.76\sigma$ and $R_B = 2.1\sigma$, indicating that binary phase segregation effects are expected to be significant for clusters of 50 atoms or more.

Neon clusters may be taken as representative of a range of quasiclassical systems. At 2.6 K ($kT/\epsilon = 0.073$) the

TABLE I. Total energy, $\langle E \rangle$, and structural properties of the $(\text{p-H}_2)_n(\text{o-D}_2)_m$ clusters. Error bars for structural quantities and $\langle E \rangle$ are $\pm 2\%$ and $\pm 1.5\epsilon$, respectively.

T (K)	m_A	m_B	n_A	n_B	$\langle E \rangle / \epsilon$	R_A / σ	R_B / σ	μ	N_A	N_B	f_A	f_B	ν
2.5	2	2	9	9	-12.8	1.51	1.51	0	4.0	4.0	1.9	1.9	0
	4	4	9	9	-22.5	1.38	1.38	0	5.6	5.6	2.7	2.7	0
	4	2	9	9	-17.6	1.26	1.60	0.24	6.0	3.8	3.7	1.4	0.56
	4	2	13	5	-19.6	1.28	1.70	0.30	5.9	3.6	4.7	0.5	1.17
5.0	4	2	9	9	-15.3	1.28	1.71	0.29	5.1	3.2	3.0	1.1	0.92

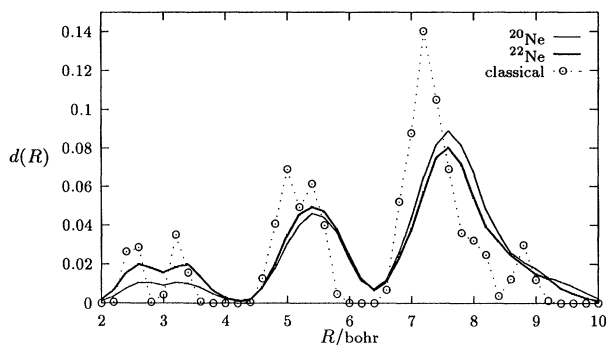


FIG. 3. Radial density profiles, $d(R)$, for the two isotopic species in $(^{20}\text{Ne})_9(^{22}\text{Ne})_9$ at 2.6 K.

10% difference in isotopic mass between ^{20}Ne and ^{22}Ne leads to λ_T values of 0.351 and 0.335, respectively, which may be compared with those for p- H_2 ($\lambda_T = 1.05$) and o- D_2 ($\lambda_T = 0.74$) at the same reduced temperature. While segregation effects are not as striking as for the p- H_2 /o- D_2 clusters, the results presented in Fig. 3 show that even in a quasiclassical system, a small mass difference can lead to well-defined structural changes. The relatively large difference in density profiles for the two species in the region from 2 to 4 bohr was reproducible in independent simulations. Results in Table II also indicate that mass segregation effects decrease with temperature.

To conclude, it has been demonstrated using FPIMC simulations that quantum delocalization effects are sufficient for isotopically mixed clusters to display a purely quantum analog of the phase separation observed in classical binary clusters. A parametric multistage sampling method for simulating binary quantum mixtures has been developed. Using this technique, it has been shown that while mass differences lead to pronounced structural consequences for strongly quantum p- H_2 /o- D_2 mixed clusters, the effects are significant even in a quasiclassical $^{20}\text{Ne}/^{22}\text{Ne}$ mixed cluster. It is evident from the results that mass effects will play as significant a role as relative binding energy or size in a variety of quasiclassical and

TABLE II. Structural properties of the neon cluster $(^{20}\text{Ne})_9(^{22}\text{Ne})_9$, as a function of temperature. The results at 2.6 K marked with an asterisk are from a classical MC simulation. Error bars are $\pm 2\%$.

T (K)	N	N_A	N_B	f_A	f_B	ν	R_A/σ	R_B/σ	μ
2.6*	6.9	6.8	6.9	3.2	3.2	0.0	1.20	1.20	0.0
2.6	6.8	6.6	7.0	3.0	3.5	0.133	1.30	1.23	0.055
5.2	6.8	6.7	6.9	3.1	3.3	0.063	1.28	1.25	0.024
10.4	6.0	6.0	6.1	2.8	2.9	0.035	1.3	1.3	0.014

quantum binary systems such as H_2/He and He/Ne mixtures. Experiments on $\text{He}_n\text{-SF}_6$ suggest that these effects may be observable for the p- H_2 /o- D_2 clusters [14,15]. For example, the introduction of a suitable chromophore (such as SF_6) in a pure p- H_2 , a pure o- D_2 , and a mixed cluster should indicate whether the interior of the cluster consists of primarily one isotopic species. Alternatively, since homonuclear diatomics are Raman active, perturbation due to the chromophore can be avoided by using Raman spectroscopic techniques for clusters [16].

Computational work presented in this paper was supported by a grant from the EPSRC, U.K. and by the Computer Sciences and Engineering Department of I.I.T.-Delhi. I would like to thank R. Ramaswamy for many useful discussions. Part of the work presented here was carried out while I was a Gulbenkian Research Fellow at Churchill College, Cambridge.

- [1] R. S. Berry, *J. Phys. Chem.* **98**, 6910 (1994).
- [2] S. K. Nayak, R. Ramaswamy, and C. Chakravarty, *Phys. Rev. E* **51**, 3376 (1995).
- [3] A. S. Clarke, R. Kapral, B. Moore, G. Patey, and X.-G. Wu, *Phys. Rev. Lett.* **70**, 3283 (1993); A. S. Clarke, R. Kapral, and G. N. Patey, *J. Chem. Phys.* **101**, 2432 (1994).
- [4] A. Belic, F. Dalfovo, S. Fantoni, and S. Stringari, *Phys. Rev. B* **49**, 15 253 (1994).
- [5] D. T. Sprague, N. Alikacem, P. A. Sheldon, and R. B. Hallock, *Phys. Rev. Lett.* **72**, 384 (1994).
- [6] D. L. Freeman and J. D. Doll, *Adv. Chem. Phys.* **78**, 61 (1990).
- [7] C. Chakravarty, *J. Chem. Phys.* **102**, 956 (1995).
- [8] C. Chakravarty, *Mol. Phys.* (to be published).
- [9] D. D. Frantz, D. L. Freeman, and J. D. Doll, *J. Chem. Phys.* **97**, 5713 (1992).
- [10] P. Sindzingre, D. M. Ceperley, and M. L. Klein, *Phys. Rev. Lett.* **67**, 1871 (1991); D. Scharf, G. J. Martyna, and M. L. Klein, *J. Chem. Phys.* **99**, 8997 (1993).
- [11] V. Buch, *J. Chem. Phys.* **100**, 7610 (1994).
- [12] The relative error for the density profiles will be minimum in the vicinity of the peaks and maximum for the tails of the distribution. Approximate error bars for the density profiles can be estimated given that the errors in the structural quantities reported in Tables I and II are $\approx 2\%$.
- [13] R. P. Feynman, *Statistical Mechanics* (Benjamin and Cummings, Reading, 1972).
- [14] K. B. Whaley, *Int. Rev. Phys. Chem.* **13**, 41 (1994).
- [15] S. Goyal, D. L. Schutt, and G. Scoles, *Phys. Rev. Lett.* **69**, 933 (1992).
- [16] V. A. Venturo, P. M. Maxton, and P. M. Felker, *J. Phys. Chem.* **96**, 5234 (1992).